Investigations of Plasma Response Associated with Resonant Magnetic Perturbation Fields in KSTAR H-Mode Plasmas

W.W. Xiao[1], T.E. Evans[2], G.R. Tynan[3], S.W. Yoon[4], Y.M. Jeon[4], W.H. Ko[4], Y.U. Nam[4], Y.K. Oh[4], and KSTAR team

1) Institute for Fusion Theory and Simulation, Department of Physics, Zhejiang University, Hangzhou, 310027, China

2) General Atomics, PO Box 85608, San Diego, CA 92186–5608, USA

3) Center for Energy Research, University of California San Diego, La Jolla, CA 92093, USA

4) National Fusion Research Institute, Joint Experiment Team, 113 Gwahangno, Yusung-Gu, 303-333, Daejeon, Korea

wwxiao@zju.edu.cn

Abstract

We report the investigations of the plasma response associated with the application of Resonant Magnetic Perturbation (RMP) fields in KSTAR H-mode plasmas using small edge perturbations produced by a modulated Supersonic Molecular Beam Injection (SMBI) during steady state RMP. The modulated SMBI provides a time varying perturbation to both the plasma density source in the region just inside the LCFS (via modulation of the neutral density) and a modulated flow damping rate (via ion-neutral charge exchange and elastic scattering). The results show that the perturbation field first excites a plasma response on the q=3 magnetic surface and then plasma response propagates inward to the q=2 surface with a radially averaged propagation velocity of resonant magnetic perturbations (V_{PRMP}) response equal to 32.5 m/s. As a result, the perturbation field brakes the toroidal rotation on the q=3 surface first causing a momentum transport perturbation that propagates both inward and outward. The propagation velocity of the resonant magnetic perturbations response on the q=2 surface is larger than the radial propagation velocity of the perturbed toroidal rotation.

1. Introduction

Large edge-localized mode (ELM) bursts in ITER plasmas are expected to release peak thermal energies about 20-30 MJ in several hundred microseconds. A big challenge is to preserve the lifetime of the plasma facing components due to the ELM-driven transient erosion. This large transient erosion has the potential to trigger plasma disruptions that can result in large thermal loads onto the first wall material, the in-vessel components and the vacuum vessel itself [1]. Based on the big challenge, a most important ELM control method, Resonant Magnetic Perturbation (RMP) fields, was demonstrated for the first time more than ten years ago [2]. Corresponding physics analyses have been reported in many significate papers [3-13], which have focused on the plasma response to 3D magnetic perturbations as well as how to control and mitigate the Large ELM bursts, even in the helium plasmas [14]. These studies have focused on the mechanisms of the RMP fields needed to control ELMs based on global effects, such as the density profile changes, resulting in a pedestal pressure decrease and a reduction in the pedestal gradient along with changes in the magnetic topology of the pedestal that impact the ELM stability.

Applied RMP fields can cause stochasticity and transport [15], however, we report the first investigations of the plasma response propagation dynamics to applied Resonant Magnetic Perturbations (RMPs) fields in KSTAR H-mode plasmas using small edge perturbations produced by a modulated Supersonic Molecular Beam Injection (SMBI) system. We show that the plasma response to the n=1 RMP in q_{95}~5.0 KSTAR H-mode plasmas is initially localized at the q=3 rational surface, where a resonant magnetic island is predicted to exists due to a weak screening by the MHD plasma response. Subsequently, the response to the RMP field is observed at the q=2 rational surface with a time delay, demonstrating the propagation of the RMP plasma response radially across the plasma. In addition, we also show that the plasma response to the RMP field results in a modification of plasma turbulence. These results provide a new understanding of how RMP fields can affect the magnetic resonant response on specific rational surfaces as well as the subsequent impact of the modified magnetic topology on the plasma turbulence and transport. RMP fields have been successfully used to control edge-localized modes (ELMs) [2] and will be used in ITER [16] in order to avoid large energy transients on the divertor produced by type-I ELMs. The mechanism of RMP control of ELMs, as originally suggested by the first

experiments [2], assumed the control of the pedestal pressure with the help of an enhanced transport in the stochastic magnetic field region formed by externally applied RMPs. Subsequently, an analysis using a linear kinetic model of RMP penetration into a plasma was developed in [17] and a quasi-linear model was introduced [18]. Here, the direct measurement of the plasma response to an applied RMP field in magnetically confined plasmas is reported for the first time. The experimental results answer the questions of "how far and how quickly" the RMP field penetrates into the plasma before triggering a change in the transport and how the transport propagates following the arrival of the RMP field on each of two primary resonant surfaces. Previous studies have relied on indirect observations of how far and how quickly the RMP penetrates into plasma [19] and on modulations of the RMP field that provide a causal connection between the plasma response and the time variations of the magnetic perturbation field [20].

In order to probe the propagation dynamics of the RMP fields in plasma [21], we actively induce perturbations in the plasma response by applying small edge plasma perturbations with a train of pulsed Supersonic Molecular Beam Injections (SMBI) [22] during a steady state RMP. The use of modulated SMBI provides a time varying perturbation to both the plasma density source in the region just inside the LCFS (via modulation of the neutral density) and a modulated flow damping rate (via ion-neutral charge exchange and elastic scattering). The resulting periodic perturbations then allows the application of transient transport analysis techniques to determine the location of the first resonant plasma response to the RMP field. Such perturbations in the plasma response to RMP can be observed by measuring the resulting changes in the plasma toroidal rotation and thus the propagation of the change in plasma response to RMP can be directly measured. The radial phase of the perturbed toroidal rotation velocity (δv_ϕ) has two minima located at the q=2 and 3 rational surfaces. Each of these phase minima represents the location of the first and the second plasma response to RMP field since the formation of a phase minima is associated with the presence of source term [23], which in this case is due to the perturbed RMP braking term in the toroidal momentum balance equation. The radially averaged propagation velocity of the RMP (V_{RMPP}) between the two rational surfaces can be thus inferred from the phase difference between the two minima since such a phase difference represents a time delay. We also show that the perturbed momentum transport

during application of the RMP is both inward and outward from the q=3 surface. In addition, the radial correlation length of the density fluctuation increases in the region around the q=3 surface with the application of RMP field.

This paper is organized as follows. Section 2 presents an overview of the experiment set-up, including the plasma condition, the frequency of the SMBI pulses, the NBI power and the operating window for the RMP combined with the SMBI pulses. Section 3 presents the experimental results and the theoretical analysis for the response of RMP field, including the phase profile of the perturbation toroidal rotation velocity during the RMP combined with the SMBI pulses, the temporal evolution of the toroidal rotation when the RMP field is applied and the theoretical analysis of the perturbation magnetic field in the plasma. Section 4 discusses the density fluctuations. The summary is presented in section 5.

2. **Experimental conditions**

The experiments were carried out in lower single null KSTAR [24] plasmas (B_T =1.6 T, I_p =0.5 MA, n_e=3.0-4.0×10^{19} m-3, R_0=1.8m, R_{sep}=2.23m). The RMP coil current was set for n=1 in the upper coil (+ + - -) with 2.40 kAt, n=1 in the middle coil (- + + -) with 2.52 kAt and n=1 in the lower coil (- - + +) with 2.46 kAt. A period of small perturbations was induced by the SMBI, which is the key small perturbation tool in this experiment. The SMBI system was installed at an equatorial port of the vacuum vessel in KSTAR. The SMBI pulses can be injected into the plasma at room temperature or low temperature. The gas pressure and pulse duration of the SMBI pulses for injection in KSTAR are from 0.4 to 2.2MPa and 8 and 10 ms, respectively. The particle number calibration curve of one SMBI pulse with temperature 105K and gas pressure 1.0MPa is shown in figure 1. Thus, the particle number of one SMBI pulse is estimated based on this curve. The neutral particle deposition of one SMBI pulse at the pedestal foot in H-mode plasma was reported in [25]. In this experiment, the parameters of the SMBI system were as follows: the frequency of the SMBI modulation is 5 Hz, the pulse duration is 6 ms and the SMBI plenum gas pressure is 0.8 MPa. The particle number of one SMBI pulse is slight less than 4 × 10^{20}. Thus, the deposition of the neutral particle induced by SMBI is shallow with small perturbations localized to the edge of the H-mode plasmas in KSTAR.

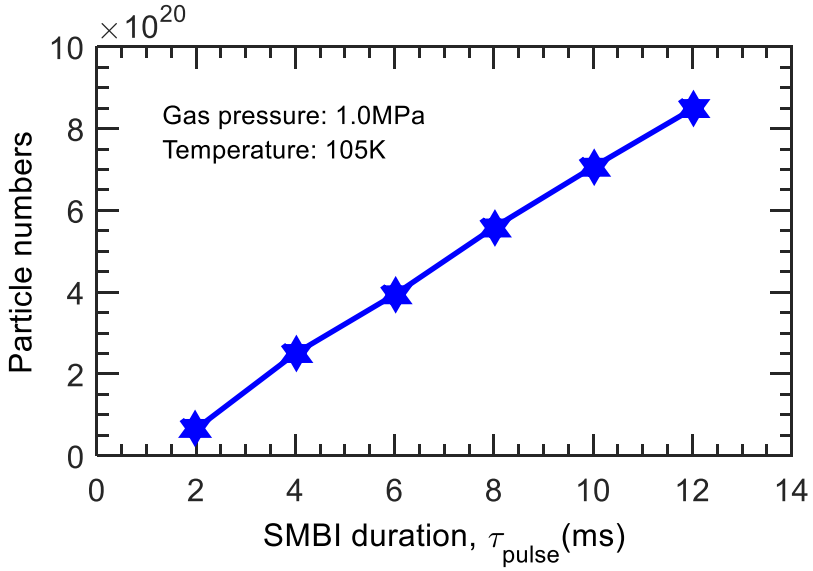

Figure 1. The particle number calibration for one SMBI pulse in KSTAR. The SMBI duration (τ_{pulse}) is the nozzle opening to closing time [22].

The discharge time is more than 11 second for shot 10884 in KSTAR. The general discharge parameters are shown in figure 2. The discharge parameters represent from top to bottom, (a) the MHD mode spectrum, (b) the Da signal, (c) the RMP coil current per turn and the SMBI pulse, (d) the line averaged density and (e) the toroidal rotation v_ϕ resolution with discharge time. Here, the RMP coil current is different at different times during the discharge. The current increases as the discharge time increase. The largest coil current is applied from 9 second to 11 second. The Magnetohydrodynamics (MHD) mode spectrum is from the Mirnov signal. In general, the frequency of the MHD spectrum decreases slightly as the current in the RMP coil increases. The MHD frequency is modulated slightly by the SMBI pulses injection during the period from 9 second to 11 second in figure 2.

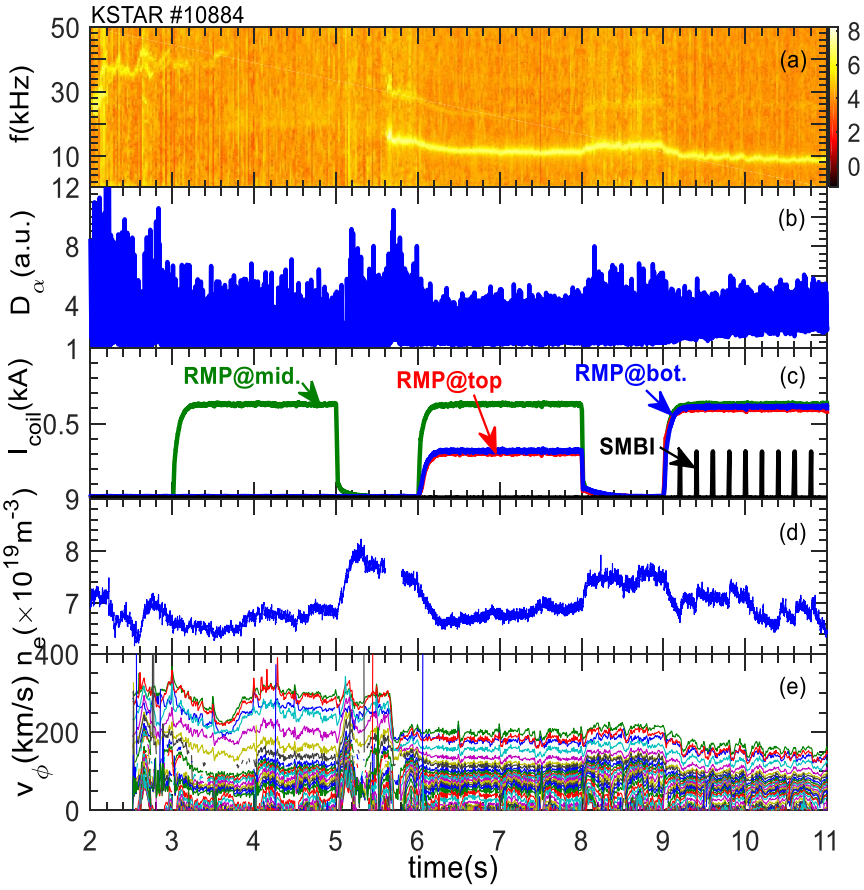

Figure 2. the discharge parameters for shot 10884. From top to bottom, (a) the MHD mode spectrum, (b) the Da signal, (c) the RMP current per turn (each coil has 4 turns) and the SMBI pulse and (d) the line averaged density and (e) the toroidal rotation resolution with discharge time.

A detailed parameter descriptions for this shot are shown in figure 3, where the focus is on the period between 9 to 11 s with the RMP and the SMBI. Here, the Neutral Beam Injection (NBI) heating power is 4.2 MW, as shown in figure 2 (a). Measurements of toroidal velocity v_ϕ of C^{+6} using Charge Exchange Spectroscopy (CES) [26] are shown in figure 3 (b), where the v_ϕ evolution with time at different spatial positions for shot 10884 is indicated. The positions of the v_ϕ measurements are at normalized radial positions ρ = 0.43, 0.7, 0.87, 0.92, 0.96. Here, the normalized radial position is scaled by minor radius *a*. Figure 3 (c) shows the spectrum of the Mirnov signal, which is noted in figure 2 (a). Based on figure 3, a clear Magnetohydrodynamics (MHD) mode with a frequency of about 11-8 kHz from 9 to 11 seconds is observed. Figure 3 (d) shows the time traces of the RMP coil current (red) and the SMBI pulsed (blue).

The MHD mode frequency and the toroidal velocity v_ϕ both were influenced by the SMBI pulse

injected, although the SMBI particle do not penetrated beyond the foot of the pedestal. The MHD mode frequency and the v_ϕ decreased very quickly once the SMBI injection, then slowly recover. We also observed, however, some accidental P_{NBI} events at 9.5s, 10.0s, 10.5s and 10.9s, as shown in figure 2 (a) by the red arrows. These accidental events are from the NBI beam drops, which influences the rotation and decreased v_ϕ abruptly at the corresponding time of the NBI power drops. It is clear that the period of the NBI are random and accidental and different from the period of the SMBI pulses (~5Hz), as shown in figure 2 (b) and (c). The influence of the NBI drops for the period of the SMBI pulses can be removed using the Fourier transform (FFT) analysis, which is similar to a filter used to eliminated the influence of the accidental NBI drops as accident cases. The details will be discussed in next section.

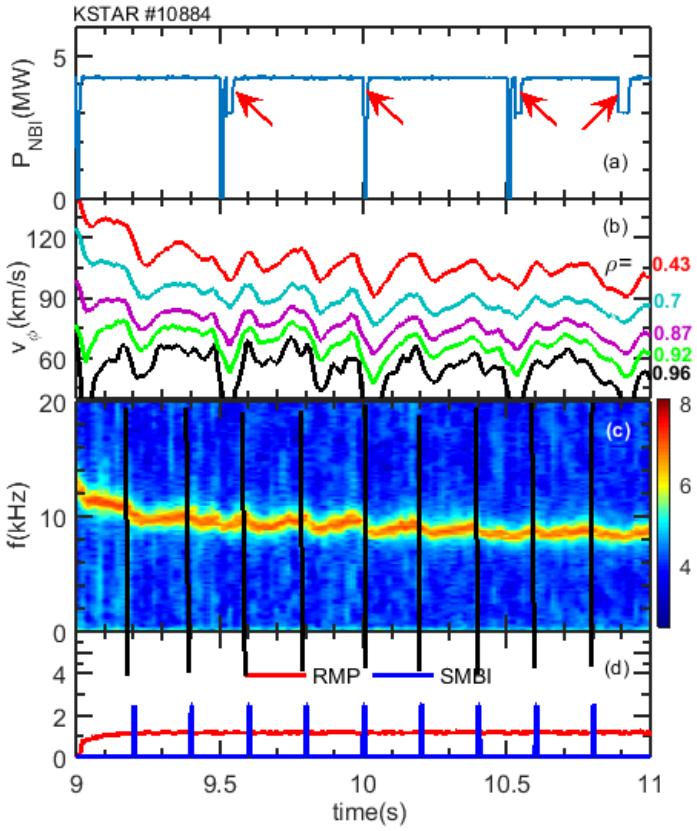

Figure. 3. (a) the NBI power is about 4.2 MW and the NBI power drops are shown by the red arrows. (b)V_ϕ is modulated by small edge perturbations from the SMBI during the steady state RMP phase. (c) is the spectrum of the Mirnov signal is shown in arbitrary unit. (d) The red curve is the current control signal of three RMP coils with ~2.4 kA and the blue pulses are the SMBI control signal.

3. The experimental results and the theory analysis

3.1 The perturbation analysis of the v_ϕ induced by the SMBI pulses

In this experiment, we used the SMBI to induce a small perturbation to explore the influence of the RMP field propagation on the plasma response (not momentum transport) since we can NOT find any other experimental method to extract this information when the RMP is held in a steady state. Here, the time delay in the plasma response to changes in the RMP field penetration are used as a proxy for the propagation of the RMP field since we are not able to made a direct measurement of the RMP field on various resonant surfaces. Thus, a small change in the poloidal rotation of the plasma will change the RMP screening factor, which can enhance the field penetration and increase the magnetic island width resulting in a measurable plasma response. This is the basis of our research approach on the propagation dynamics, related to the impact of the RMP fields on the particle, heating and momentum.

Based on the experimental data, there are few accidental events of the NBI power drops during the SMBI pulse injection from 9 s to 11 s, especially at about 10.0s. Thus, the FFT analysis method is very important and effective for reducing or removing the influence of the accidental perturbation events from the NBI since if we only focus on one SMBI pulse propagation, the accidental NBI power drop will induce a large influence for the propagation analysis. Actually, when we do the FFT analysis for all SMBI pulses, the one NBI pulse influence at about 10 s will be reduced since this one is a noise source in the FFT analysis. Basically, the most effective use of the FFT analysis is to remove noise sources in the data analysis. In the experiment, for the FFT analysis of the SMBI period, we know the frequency of the SMBI is 5Hz, while the accidental NBI power drop frequency is about 2Hz in the period from 9 second to 11 second. The accidental NBI power drops can't be actively controlled by the experimental design. However, the SMBI period 5Hz can be actively controlled. In this way, the 5Hz of the SMBI pulses is our useful experimental signal for the perturbation method. Finally, we can filter and reduce the influence of the accidental NBI power drops used in the SMBI perturbation analysis.

Detailed results of the FFT analysis for the perturbation of v_ϕ at different radial positions in the plasma are shown in figure 4 (a) and figure 4 (b). The FFT results for v_ϕ at ρ=0.43 and ρ=0.7 can be observed, which is induced by active SMBI injection. This is the useful signal for the perturbation analysis in the experiment, while the effect of the SMBI pulses almost disappears

at the edge plasma, as shown in figure 4 (c). The window for the FFT analysis is from 9.18 s to 11.0 s, including all SMBI pulses in this shot. Based on the results, as shown in figure 4, we do not observe the NBI frequency during the SMBI injection period from 9 to 11 seconds. Thus, we can ignore the accidental events from the NBI power drops.

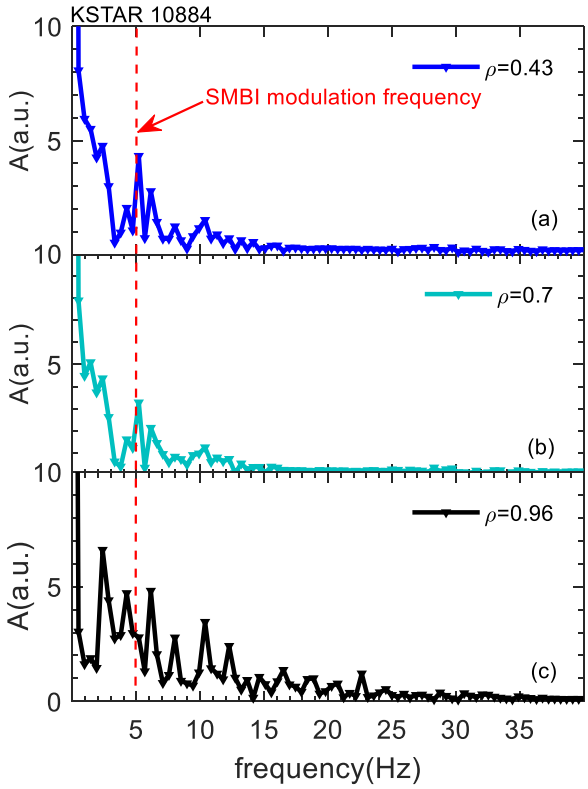

Figure 4. Perturbation analysis using the FFT method for the v_ϕ at different radial positions. The red dashed line represents the 5 Hz of the SMBI pulses modulation frequency. The modulation effect of the SMBI pulses almost disappeared at the edge plasma, as shown in this figure (c).

The small perturbations of v_ϕ were induced by the SMBI pulses as mentioned above, and as shown in figure 3 and figure 4. We applied the purbative transport analysis method [23] based on Fourier transform (FFT) for $v_\phi(t)$ at each normalized radius and extracted the propagation characteristics of perturbed v_ϕ, which is shown in figure 5. Figure 5 (a) shows the safety factor (q) profile, which is important for determining the resonant location of the RMP [20, 21]. The phase profile of the perturbed v_ϕ is shown in figure 5 (b) where the SMBI modulation is used as the phase reference. We emphasize that there are two phase minima. One is at q=2 located at ρ = 0.42 and another is at q = 3 located at ρ = 0.7, as seen in figure 5 (b). In perturbative plasma

transport experiments, a minimum phase position generally indicates the position of an induced perturbation source [23, 27, 28]. The induced minimum phase in v_ϕ is unlikely to be due to a modulation of the "neutral particle source" because SMBI neutral particles cannot penetrate through the edge plasma to reach the q=3 position, let alone q=2 positions in KSTAR H-mode discharges [22] and would not result in the localized minima seen at q = 2 and 3. We also discussed the neutral particle deposition in section 2 for a shallow neutral particle deposition induced by SMBI. Thus, the perturbation source in the plasma, corresponding to the minimum phase location, must be induced by a difference in plasma response due to the RMP field. Comparing figure 5 (a) and (b), we see that the phase minima are close to the q=3 and q=2 rotational surfaces, as shown by the red bars. The phase difference ($\Delta\phi$) ~ 0.11 rad, denoted by the vertical arrows in figure 5 (b), between two locations at q=3 to q=2 indicates the propagation delay associated with a first responses at the q = 3 surface, followed by the response at the q=2 rational surface. This indicates that there is a time delay of the effect of the RMP field on the transport from q=3 to q=2 [21]. These experimental results support the current RMP physics hypothesis being used for ITER, which states: *"The RMP coils are shown to induce a layer of stochastic magnetic fields near the last resonant magnetic surface, typically q = 3 in the tokamak" [29].*

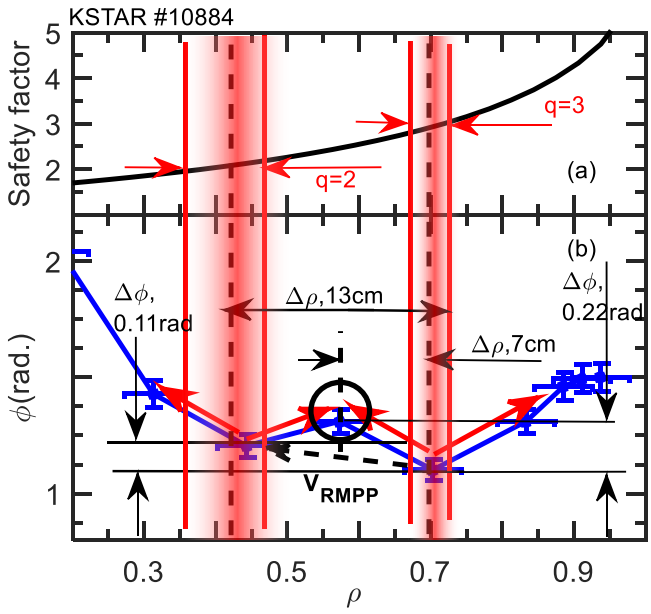

Figure 5 (a) the safety factor profile and (b) the phase profile of the perturbed v_ϕ as shown by the blue curve. The vertical double red lines and the red bars represent the uncertainties of the safety

factor profiles and the minimum phase locations, respectively. The dashed lines indicate the locations of the q=3 and q=2 rational surfaces separated by 13 cm. The black circle will be discussed in section 3.4.

Although, no phase minima are observed when the modulated SMBI is applied without the RMP in KSTAR H-mode plasmas, there is a uniform reduction in the rotation profile due to the edge localized drag from the SMBI [22]. Thus, the presence of the RMP field in plasma and the presence of a phase minima in the plasma response to the RMP field can be uniquely determined by using small edge perturbation caused by SMBI pulses. As expected from our guiding idea envisioned for the experiment, we measured a clear first response originating on the q=3 surface, which we presumed is the location near the zero crossing of the perpendicular electron E×B rotation frequency [30]. In addition, we see a radial propagation of the changing rotation from the q=3 point of origin both inward and outward with a subsequent change in the rotation profile at q=2 as shown in figure 5. Our physics hypothesis for this change in the RMP field originating at the q=3 and shortly afterwards at q=2 surfaces is that the SMBI creates a drag on the edge plasma. The scenario envisioned here is that the drag from the SMBI pulses causes a change in the electron poloidal E×B and diamagnetic flow near the q=3 rational surface which reduces the resonant field screening and allows a larger magnetic island to form. The larger q=3 magnetic island causes an additional drag on the poloidal flow [31], which subsequently results in a reduction of the resonant screening on the q=2 surface. We described our physics conclusion as a hypothesis since there is no a direct measurement of an increase in the magnetic island size on the q=3 surface or the q=2 surface. We prefer to remain conservative on this point until we can make a direct measurement of the changes in the islands on the q=3 and 2 surfaces. We hope to be able to extend our results in the future on KSTAR by making measurements in the q=3 and q=2 islands using the Electron Cyclotron Emission (ECE) and ECE imaging (ECEI) [32] diagnostics to observe the T_e flattening and phase inversion associated with these magnetic islands.

3.2 The Radially averaged propagation velocity of the RMP field

A speed of the propagation can be determined by a displacement and the time in the

displacement. As we know, it is very difficult to measure the resonant locations of the perturbation magnetic field inside the high temperature plasma using the experimental method, expect by carrying out a theoretical analysis. The main difficulty is not only the high temperature, but also the fact that there is no diagnostic tool to "see" the perturbation magnetic field in the plasma. In order to trace the propagation velocity of the perturbation field in the plasma, an active small perturbation was performed using SMBI pulses at the plasma edge during a steady state RMP field in this experiment. This small perturbation at the plasma edge will cause a change in the electron poloidal EXB and diamagnetic flow which reduces the resonant field screening. In other words, a change in the coupling of the RMP field to the resonant surfaces in the plasma is induced by the SMBI. In this way, based on figure 5 one can calculate the propagation distance and the time during the corresponding distance. First, we will calculate the time associated with the propagation distance of the RMP field. A time delay for the propagation of the RMP resonance to move from the q = 3 to q = 2 surfaces, given by $\Delta t = \Delta\phi/\omega = \Delta\phi/(2\pi \cdot f)$ Hz^{-1}, can be calculated using the $\Delta\phi$ and the f. Here, f is the modulation frequency of the SMBI (5Hz) and $\Delta\phi$ is the phase delay of the RMP propagation from the q = 3 to q = 2 surfaces, which is 0.11 rad corresponding to $\Delta t = 4\times10^{-3}$ s. Thus, Δt is about 4ms. This experimental result agrees with a modeling study result presented in [33] where the estimated RMP propagation time is shown to be on the milliseconds time scale. Second, we will calculate the propagation distance of the RMP field. The radial mid plane distance from the rational q = 3 to q = 2 surfaces is $\Delta\rho\times(R_{sep}-R_0) \sim 0.3\times(R_{sep}-R_0) = 0.13$ m based on the machine scale. Then, the radial averaged velocity of the RMP field (V_{RMPP}) in H-mode plasma may be obtained using the distance and the time delay. V_{RMPP} is shown in figure 3 by the black dashed arrow with an inward propagation velocity of 32.5 m/s. The change related to the momentum transport in the toroidal phase response of v_ϕ is calculated in a similar way. One can define the radial propagation velocity of V_ϕ away from the q = 3 as $v_{\phi p}$ using $\Delta r/\Delta t$. Here, the Δr is about $0.15\times(R_{sep}-R_0) = 0.07$ m and Δt is $\Delta\phi/(2\pi \cdot f)$ Hz^{-1} $\sim 0.22/(2\pi \cdot 5)$ $Hz^{-1} = 7\times10^{-3}$ s, as shown in Fig. 5 (b) where Δt is the time needed for the v_ϕ disturbance to propagate. Thus, the $v_{\phi p}$ is about 10 m/s from the q=3 resonant surface to the point approximately half way between the q=2 and q=3 resonant surfaces, as shown in figure 5 (b) by the red arrow. This indicates that the momentum transport of the perturbation v_ϕ is induced by the small perturbation of the SMBI when the RMP field is present. We note that

V_{RMPP} is faster than the $v_{\phi p}$ in the region between the q=3 to q=2 rational surfaces. This means that the RMP field influences the plasma on faster time scale than the radial propagation velocity of the v_ϕ related to the momentum transport. The ion sound speed, c_s, can be calculated using the $c_s=9.79\times10^5(\gamma ZKT_e/\mu)^{1/2}$ with $\gamma=2$, Z=2, $\mu= m_i/m_e = 2$ and $T_e=1$keV, then $c_s \sim 1.4\times10^3$ m/s. Thus, V_{RMPP} is about 2 orders of magnitude smaller than the ion sound speed. It is also much slower that the Alfven speed (2.9×10^5 m/s) indicating that it may be associated with a change in the Neoclassical Toroidal Viscosity (NTV) associated with a change in the non-resonant eigenmodes of the applied 3D field from the RMP coil [34] when the SMBI is applied. Here, the Alfven speed is $V_A = 2.18\times10^{11}\mu^{-1/2}n_i^{-1/2}B_t$ with $\gamma=2$, $n_i=6\times10^{13}$ cm^{-3}, $B_t =1.5\times10^4$ Gauss. Therefore, based on the comparisons, the V_{RMPP} is slower than the ion sound speed and also much slower that the Alfven speed, while V_{RMPP} is little bit faster than the $v_{\phi p}$ (radial propagation velocity of the v_ϕ) related to the momentum transport in same time scale.

3.3 The temporal evolution of the v_ϕ with and without RMP field

The temporal evolution of the toroidal rotation when the RMP field is present can be seen in figure 6 (a). The results show how the rotation profile changes as a function of time following the application of the RMP field at t = 9.0 s and demonstrates the importance of the RMP fields on the q=3 rational surface. In figure 6 (b), $v_\phi(0)$ (black) is an averaged profile of the toroidal rotation just before the RMP is applied from 8.9s to 9.0s, and the $v_\phi(t)$ is the toroidal rotation profile at different times with RMP. The q=3 rational surface and the pedestal top are denoted by black and red vertical dashed lines, respectivley. It can be clearly seen in figure 6 (a) that the braking in v_ϕ occurs strongly around the q=3 rational surface following the application of RMP statring from t= 9.0 s, altough the braking is further enhanced and transiently spreads inward and outward following the SMBI pulse at t=9.2 s. A more detailed analysis of the induced V_ϕ braking by the RMP field is shown in figure 6 (b). The black curve is the v_ϕ profile without RMP at t = 8.9 s, the red curve is with the RMP at t = 9.15 s and the blue curve is the difference between the black and the red curves (multiplied by a factor of 8). Figure 6 (b) clearly shows that the largest change in v_ϕ occurs at ρ = 0.7, which corresponds to the location of the q = 3 rational surface, showing that the v_ϕ braking occurs aournd the q = 3 rational sureface, as shown in figure

6 (b) by the red arrow. This v_ϕ braking induces the propagation of the toroidal momentum inward and outward from the resonant location, as shown in figure 6 (b) by the blue arrows. We emphasize again that the presence RMP is required for the localized braking as shown in figure 6. In contrast, without the RMP, applying SMBI only led to a uniform reduction in toroidal rotation without a localized v_ϕ braking around the rational surface [22].

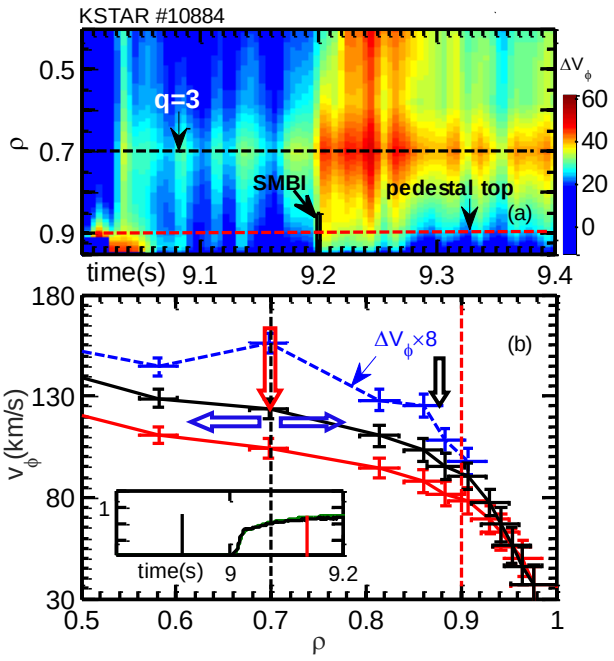

Figure 6. (a) Δv_ϕ as a function of time following the application of the RMP field. (b) the v_ϕ profiles without and with RMP for shot 10884 as shown using the black curve and the red curve, respectively. The Δv_ϕ x 8 is shown as blue dashed line. The inner small box represents the RMP time trace, and the black vertical line and the red vertical line in the small box indicate the time points of the v_ϕ profiles obtained at 8.9 s and 9.15 s, respectively.

3.4 The theory analysis of the perturbation magnetic field in the plasma

An analysis of the RMP spectrum via vacuum superposition for shot 10884 at 10.0s is shown in figure 7. The color bar indicates the intensity of the perturbation amplitude of the RMP. According to this figure, although it is vacuum superposition, the applied n=1 RMP field is resonant on each of the m/n rational surfaces from m=1 to m=7 in this charge. We also can see that there is a gap in the peak RMP amplitude around the normalized flux from 0.45 to 0.52, as shown by the red circle in figure 7. This indicates that there is reduction in the non-resonant

eigenmode perturbation amplitude of the RMP from the plasma edge to the core. In other words, there are two strong regions of non-resonant RMP field based on the discontinuous intensity profile. The discontinuous intensity profile phenomena was also observed in EAST [35]. In figure 7, the gap or the discontinuous intensity profile of the perturbation amplitude of the RMP (as shown by the red circle) is consistent with a bulge at ρ ~0.58 of the phase profile of the perturbation v_ϕ in figure 5 as shown by the black circle. Thus, theoretical analysis of the RMP spectrum is consistent with the experimental results. This means that the theoretical analysis and the experimental results support the experimental results showing that there are two resonant locations of the RMPconnected by a discontinuous non-resonant field in the vacuum f ield that are likely to be altered by the change in the boundary conditions imposed bey the SMBI pulses. The error of the positions between the gap of the theoretical analysis of the RMP spectrum and the bulge of the phase profile of the perturbation of v_ϕ results from the difference between the experiental measurment and theoretical boundary setup. The key point is that there is a non-continuous change of vacuum RMP field in the plasma. In other words, there is a non-monotonic profile of the phase in the toroidal rotation as observed in the experiment. In addition, the results of the theoretical analysis from the DIII-D [20, 36] and the KSTAR [27] also show that there are two changes in the perturbation amplitude of the RMP near the rational surfaces.

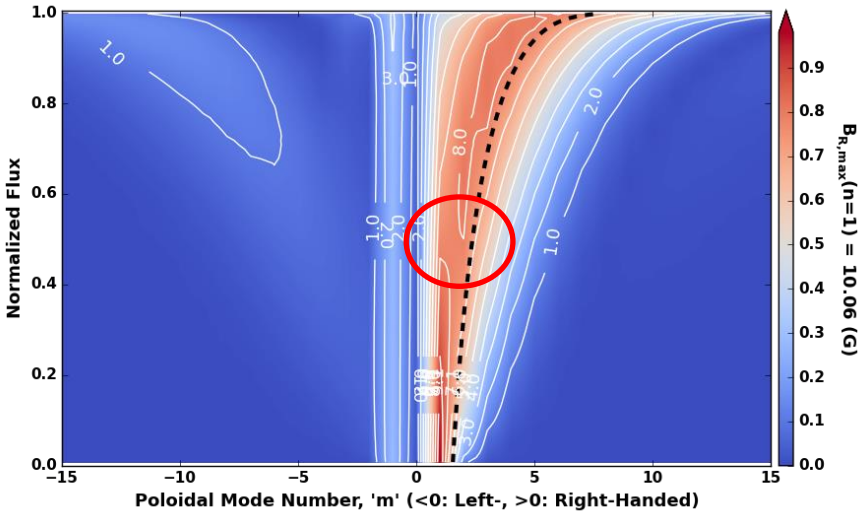

Figure 7. Contour plot of Contour plot of Br(m,1) for vacuum superposition for shot 10884 at 10.0s based on the equilibrium. The color bar indicates the intensity of the perturbation

amplitude of the RMP. There is a reduction as shown by the red circle. The gap or the discontinuous intensity profile of the perturbation amplitude of the RMP as shown by the red circle is consistent with a bulge at ρ ~0.58 of the experimentally measured phase profile of the perturbation v_ϕ in figure 3 as shown by the black circle.

4. The density fluctuations analysis during the RMP and the SMBI

Density fluctuations induced by the SMBI were reported in KSTAR [22]. The edge density fluctuations was measured by beam emission spectroscopy (BES) [37] (BES channel 6 at R = 2.277 m, the R_{LCFS} = 2.278). In figure 8, the blue curve and the red curve show the analysis of results without and with SMBI, respectively. The obvious difference is that the low-frequency content of the edge density fluctuation spectrum decreases, while the higher frequency content increases as the basic mechanism of the ELM mitigation using the SMBI injection. The mechanism of the ELM mitigation using the SMBI have been reported since the ELM mitigation results from an increase in higher frequency fluctuations and transport events in the pedestal caused by SMBI, and inhibit the occurrence of large transport events which span the entire pedestal width [25].

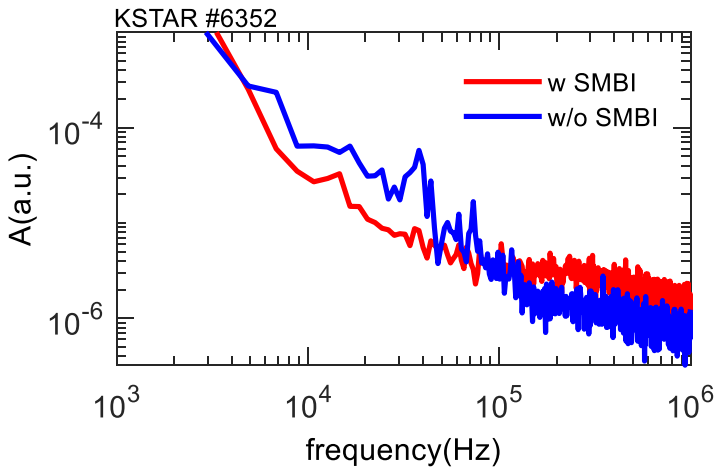

Figure 8. Comparison of the density fluctuation obtained from BES for shot 6352 in the pedestal region for the ELM mitigation. The SMBI influence time is more than 300 ms.

The SMBI parameters for the ELM mitigation using the SMBI are: duration is 10ms, the gas pressure is 1MPa and the gas temperature is 104k. The SMBI influence time, τ_I, is longer than 300 ms for shot 6352 in KSTAR. Here, the SMBI influence time τ_I is defined as the time interval

during the Dα amplitude decrease or disappearance to the first Dα amplitude recovery. The experimental design for research into RMP propagation dynamics, uses SMBI injection induce small perturbation during steady state RMP field. As reported on ELM mitigation using the SMBI, the SMBI influence time is more than 300 ms. This is not the basis of our proposal on research for understanding RMP propagation dynamics. Here, we designed the experiment to show that the small perturbation induced by the SMBI during the steady state RMP field can provide the information needed to understand the RMP impact on the plasma. Thus, we used the SMBI pulse parameters with a duration of 6 ms, a gas pressure of 0.8 MPa at room temperature, to induce small perturbations at the plasma edge. In this case, the SMBI influence time, τ_I, is about 12 ms, as shown in figure 9(a). This τ_I time scale is used for our RMP field propagation research since it is much short than that in ELM mitigation using SMBI injection. Thus, the SMBI parameters, especially the gas temperature, are different in the two different experiments.

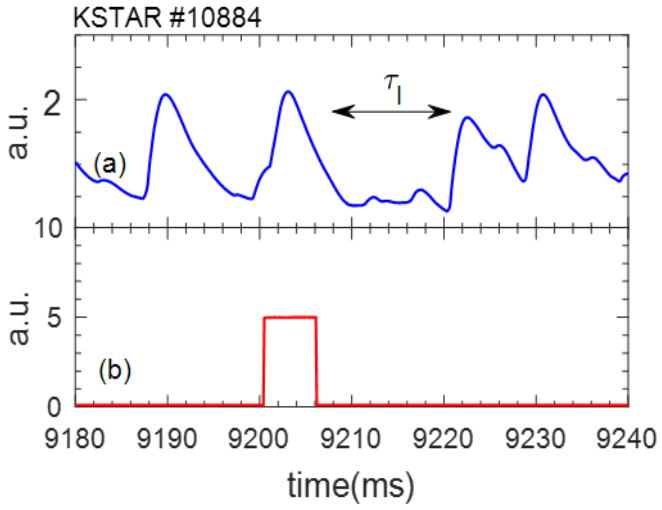

Figure 9. The edge small perturbation was induced by the SMBI pulses during the steady state RMP field. The SMBI duration is 6ms, the gas pressure is 0.8MPa with room temperature. The SMBI influence time is about 12ms.

In addition to braking toroidal rotation, RMP has also been shown to induce changes in plasma turbulence and thus local transport. Here, we compare the radial density fluctuation profiles with and without RMP using the 4×16 BES arrays in KSTAR. The analysis range of the BES measurements in the experiments is from -5.1 cm to -13.8 cm below the mid plane and from the separatrix to a distance 12cm inside of the plasma. The density fluctuations can also be changed

by the SMBI pulses injection, as has been reported in our previous work on the ELM mitigation by the SMBI [19]. In order to avoid the influence of the SMBI injection on the turbulence analysis, two special time windows for turbulence analysis were chosen: the time window without RMP is from 9.0-9.006 s, and the time window with RMP is from 9.7-9.706 s, which is far from the SMBI injection time. A basic measurement of the density fluctuations by the BES system is shown in figure 10 at at ρ~1.0 position. In this figure, the blue curve and the red curve show the analysis of results without and with RMP, respectively. This is very similar to the case of the ELM mitigation using SMBI injection: the low-frequency content of the edge density fluctuation spectrum decreases, while the higher frequency content increases slightly when the RMP field was applied into the plasma.

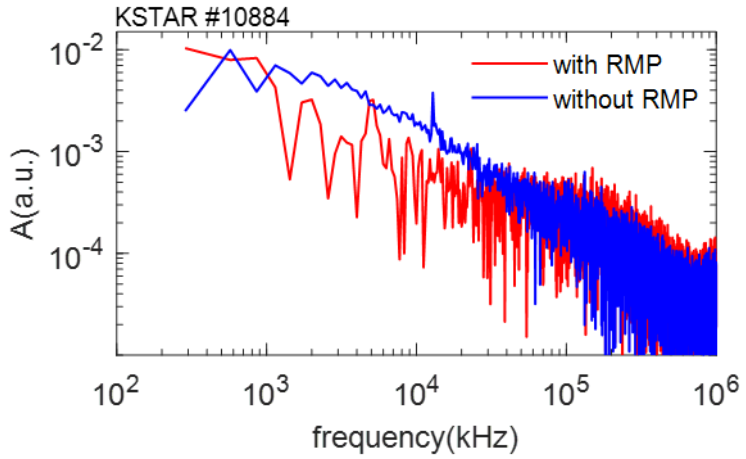

Figure 10. The density fluctuation measured by the BES at ρ~1.0 position for shot 10884. The red curve shows the density fluctuation with RMP from 9.7-9.706 s and the blue curve shows the density fluctuation without RMP from 9.0-9.006 s.

In order to observe a wider region change of the density fluctuation, the radial correlation length of the density fluctuation with and without the RMP was analyzed using BES for shot 10884, as shown in figure 11. Here, the *1/e* coherence value is designated as the radial correlation length (L_r) [38]. The radial measurement range is inward beginning from the pedestal top, which is the reference point located at the pedestal top for the coherence (γ). With the RMP, L_r increases from 1.4 cm to 2.2 cm for fluctuations with f >30 kHz (denoted ambient turbulence, AT) and increases from 2.6 cm to 3.2 cm for fluctuations with f <30 kHz (denoted low frequency turbulence, LFT), as shown in figure 11 (a) and (b), respectively. This means that there are no SMBI pulses during

the time windows of the turbulence analysis. This shows that the density fluctuation radial scale length increases with the application of a steady state RMP. This is consistent with the turbulence causing additional radial transport during the RMP [39]. The increased turbulence and v_ϕ braking produced by the RMP result in the reduction of the pedestal toroidal rotation (figure 3 (b) by the black arrow).

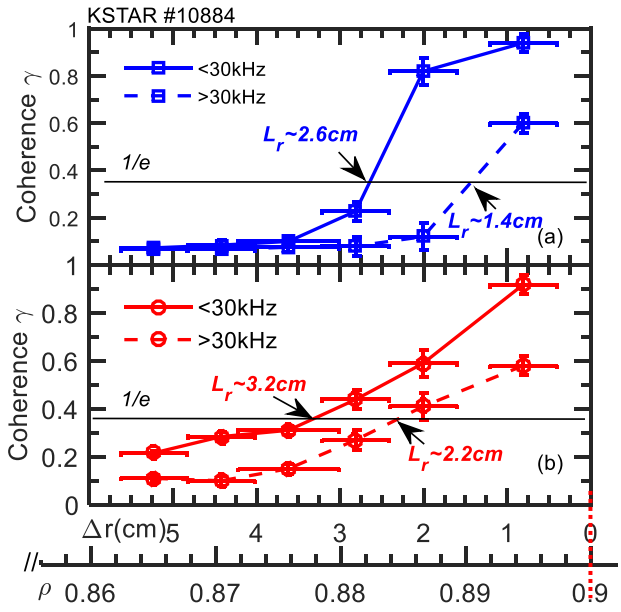

Figure 11. (a) the coherence coefficient (γ) profiles and radial correlation length (L_r) without RMP during 9.0-9.006 s and (b) the same as in (a) but with RMP during 9.7-9.706 s. No SMBI pulses were injected during the time windows. The position of the pedestal top is at $\rho = 0.9$, as shown by the red dot line.

5. Conclusions and Discussions

We report the first investigations of the plasma response propagation dynamics of Resonant Magnetic Perturbations (RMPs) fields in KSTAR H-mode plasmas using small modulated edge perturbations produced by a Supersonic Molecular Beam Injection (SMBI) system during the steady state RMP regime. The experiments demonstrate that the RMP penetrates the pedestal region where it first resonates at the q=3 rational surface and then at the q=2 rational surface. From the q=3 rational surface to q=2 rational surface, the radial averaged velocity of the RMP plasma response to the change in the penetration of the perturbation field (V_{RMPP}) in the H-mode

plasma is about 32.5 m/s, which is much slower than either the ion sound or Alfven velocity but more than 4 times faster than the radial propagation of the change in the toroidal rotation. The RMP field resonates at the rational surface, brakes the toroidal velocity v_ϕ, induces the propagation of the toroidal momentum inward and outward from the resonant location, and increases the density fluctuation, which finally results in a reduction of the pedestal toroidal rotation. A theoretical analysis of the RMP spectrum via vacuum superposition for shot 10884 at 10.0s based on the equilibrium shows that there is a gap or a discontinuous intensity profile of the non-resonant amplitude of the RMP in figure 7, which is also consistent with a bulge at ρ ~0.58 of the phase profile of the perturbation v_ϕ in figure 5.

Density fluctuation radial correction length increase during the RMP phase, similar to the density fluctuation change with the SMBI pulses injection in ELM mitigation experiments. In order to avoid the influence of the SMBI injection on the turbulence analysis, two special time windows for turbulence analysis were chosen. A wider region of the density fluctuations is researched using the analysis of the density fluctuation radial scale length. It indicates that the density fluctuation radial scale length increases with application of a steady state RMP. This is consistent with the turbulence causing additional radial transport during the RMP. The increased turbulence and v_ϕ braking produced by the RMP result in the reduction of the pedestal toroidal rotation. These new results provide further physical insight needed to refine our knowledge related to the physics of RMP propagation dynamics and ELM control using RMP in H-mode plasmas and extend the current understanding of the RMP physics required for developing reliable ELM control in ITER.

It should be noted that two important physics topics are highlighted by the experiment of the propagation dynamics associated with resonant magnetic perturbation fields in KSTAR H-Mode plasmas, the RMP plasma response propagation velocity from the q=3 rational surface to the q=2 rational surface and the perturbation field braking of the toroidal rotation on the q=3 surface first causing a momentum transport perturbation that propagates both inward and outward. The physics issues connected with this experiment could be improved in the future:

(i) The real process of RMP plasma response propagation in the plasma is a complex in experiments because of the toroidal plasma rotation such that even the small

perturbations induced by the supersonic molecular beam injection (SMBI) could reduce the influence of these small perturbations in the plasm edge. Thus, it is very important to focus on the plasma response propagation dynamics of the RMP field in the core plasma, such as from the rational surface q=3 to the rational surface q=2. However, in this case, we can only get the averaged velocity of the RMP field in the plasma. Indeed, it is very difficult to get the accurate and detailed process of the changes in the RMP field penetration from the q=3 to q=2 in the experiments. Thus, a theoretical analysis can provide key points for understanding the physics responsible for our results in more detail. We also believe that it is necessary to improve the measurement results based on the higher spatial and time resolutions in order to assess the key physics issues.

(ii) In order to more accurately determine the properties of the global propagation dynamics of the RMP plasma response from the plasma edge to the core, it is also worthwhile to explore the existence of the relatival minimum phase of the toroidal rotation velocity in the plasma edge if possible. However, the experimental error of the measurement in the edge plasma or in the pedestal region is very large, which makes this quite difficult. The possible reasons that may cause the large error in the plasma edge are as following:

(1) the small perturbation induced by the SMBI and the complex turbulence transport including the ELM bursts in the pedestal region can influence the perturbation analysis.

(2) the steep edge safety factor profile (q profile) in this narrow region is another limiting factor for the experimental measurements as well as the possibility of a small plasma shift which will induce a large error.

Thus, experimental diagnostics with higher spatial resolution used for the local measurements are needed to improve and to explore the global propagation dynamics of the RMP plasma response from the plasma edge to the core.

(iii) As a general remark, the RMP fields always has resonant and non-resonant components. The resonant components propagate on the several ms timescale, as concluded from the experimental research, while the non-resonant components are expected to penetrate on a much faster timescale so this is an open and important topic for the RMP field propagation dynamics. More importantly, the non-resonant component can also damp the plasma toroidal flow via NTV. Currently, we do not have any experimental data to make

comments on the NTV torque effect in these experiments. We would need to do either an ideal or resistive MHD simulations of the plasma to see how important the non-resonant (NTV) response is in this case. Normally, we expect the non-resonant MHD response to depend on the plasma beta. In conventional aspect ratio tokamaks like KSTAR the non-resonant MHD response increases with beta-normal. In addition, we expect the NTV torque density to be peaked near the edge of the discharge, which will affect the edge rotation more that the core rotation (for example at q =2). This is another important topic to be looked at with ideal MHD simulations with a code like MARS-F or IPEC/GPEC in a future experiment with improved profile data.

This work was supported in part by the US Department of Energy under DE-FG02-08ER54999, DE-FC02-04ER54698 De-FG03-97ER54415, DE-FG02-89ER53296, DE-FG02-07ER54917, DE-FG02-07ER54917, DE-AC02-09CH11466, DE-SC0001961, DE-SC0012706, DE - SC0018030 a 2016-17 General Atomics contract from the National Fusion Research Institute and the National Natural Science Foundation of China under Nos. 11875234 and 11575055.

References

[1] Evans T.E. et al 2017 Nucl. Fusion 57 086016

[2] Evans T.E. et al 2004 Phys. Rev. Lett. 92 235003

[3] Fenstermacher M.E. et al 2008 Phys. Plasmas 15 056122

[4] Suttrop W. et al 2011 Phys. Rev. Lett. 106 225004

[5] Orlov D.M. et al 2012 Fusion Eng. Design 87 1536

[6] Evans T.E. et al 2013 Nucl. Fusion 53 093029

[7] Jeon Y.M. 2012 Phys. Rev. Lett. 109 035004

[9] Liang Y. et al 2007 Phys. Rev. Lett. 98

[8] Kirk A. et al 2010 Nucl. Fusion 50 034008

[10] Evans T.E. et al 2008 Nucl. Fusion 48 024002

[11] Snyder P.B. et al 2012 Phys Plasmas 19 056115

[12] Wade M.R. et al 2015 Nucl. Fusion 55 023002

[13] Moyer R.A. et al 2005 Phys. Plasmas 12 56119

[14] T.E. Evans et al 2017 Nucl. Fusion 57 086016

[15] Rechester A.B. and Rosenbluth M. N. 1978 Phys. Rev. Lett. 40 38

[16] Loarte A. et al 2003 Plasma Phys. Controlled Fusion 45 1549

[17] Heyn M.F. Ivanov I.B. Kasilov S.V. and Kernbichler W. 2006 Nucl. Fusion 46 S159

[18] Heyn M.F. et al 2013 Problems of Atomic Science and Technology, Plasma Physics Series 1 (North Holland, Amsterdam) Vol. 83 p. 51.

[19] Kirk A. et al 2010 Nucl. Fusion 50 034008

[20] Xiao W.W. et al 2016 Nucl. Fusion 56 064001

[21] Xiao W.W. et al 2017 Phys. Rev. Lett. 119 205001

[22] Xiao W.W. et al 2014 Nucl. Fusion 54 023003

[23] Lopes Cardozo N.J. 1995 Plasma Phys. Control. Fusion 37 799

[24] Yoon S.W. et al 2011 Nucl. Fusion 51 113009

[25] Xiao W.W. et al 2012 Nucl. Fusion 52 114027

[26] Ko W.H. et al 2010 Rev. Sci. Instrum 81 10D740

[27] Xiao W.W. et al 2010 Phys. Rev. Lett. 104, 215002

[28] Zhong W.L. et al 2013 Phys. Rev. Lett. 111 265001

[29] Horton C. and Benkadda S. 2015 ITER Physics, Chapter 6, p 156, World Scientific Publishing Co. Pet. Ltd, Singapore

[30] Ferraro N. M. et al 2013 Nucl. Fusion 53, 073042

[31] Chu M.S. et al 2011 Nucl. Fusion 51 073036

[32] Yun G.S. et al 2010 Rev. Sci. Instrum 81 10D930

[33] Liu Y.Q. et al 2013 Phys. Plasma 20 042503

[34] Shaing K. C. 2003 Phys. Plasmas 10 1443

[35] Li J.G. et al 2013 Nat. Phys. 9 817

[36] Orlov D. M. et al., 2016 Nucl. Fusion 56 036020

[37] Nam Y.U. et al 2012 Rev. Sci. Instrum. 83 10D531

[38] Schirmer J. et al 2007 Plasma Phys. Control. Fusion 49 1019-1039

[39] Mckee G.R. et al 2013 Nucl. Fusion 53 113011